4ICEGE Thessaloniki-GREECE 2007

4th International Conference on
Earthquake Geotechnical Engineering
June 25-28, 2007
Paper No. 1119

LIQUEFACTION MITIGATION OF SAND DEPOSITS BY GRANULAR PILES: DENSIFICATION AND DILATION EFFECTS

Madhira R MADHAV [1], Murali Krishna ADAPA[2]

ABSTRACT

The paper presents and summarises comprehensively the drainage, densification and reinforcement effects of granular piles in liquefaction mitigation. Liquefaction mitigation of the ground treated by granular piles (GP) is assessed considering the pore pressure generation and dissipation taking into account the densification and dilation effects along with drainage effect. Model of pore-water pressure generation and dissipation developed by Seed and Booker (1977) is applied, with some modifications for the densification and dilation effects of GPs, in terms of modifications in coefficients of volume change and permeability and generation of negative pore pressures due to dilatancy, to the analysis of columnar gravel drains under a variety of earthquake conditions. The combined effects of densification and dilation of the granular piles are proved to be more effective in mitigating the liquefaction potential of sand deposits.

Keywords: Ground improvement, Granular piles, Liquefaction, Drainage, Dilation, Densification.

INTRODUCTION

Seismic hazards date from many centuries. Earthquakes are constantly posing risk to life and infrastructure facilities. Seismic hazards can be described by ground shaking, structural hazards, liquefaction, landslides, failure of earth structures, lifeline, tsunami and seiche hazards. One of the most dramatic causes of damage to structures during earthquakes has been the development of liquefaction in loose saturated sand deposits, manifested either by the formation of boils and mud-spouts at the ground surface, by seepage of water through ground cracks or in some cases by the development of quick sand conditions over substantial areas (Seed and Idriss 1982). Soil liquefaction is the state at which the soil deposit looses its strength and flows as a fluid A qualitative understanding of the mechanism underlying the liquefaction of saturated sands, subjected to cyclic loading, such as that induced by earthquakes, had been recognized widely since first being examined by Casagrande in 1936 (Martin et al. 1975).

Saturated granular material, when subjected to cyclic loading involving the reversal of shear stress, tends to compact or densify. Under undrained conditions, in cases where the soil consists of loose granular materials and high water table, the tendency to get densified may result in the development of excess hydrostatic pore water pressure during each cycle of loading. If the magnitude of pore-water pressure generated equals the confining pressure, the effective stress becomes zero, the soil is said to have liquefied. Pore pressure buildup leading to liquefaction may be due to static or cyclic stress applications and the possibility of its occurrence depends on the void ratio or relative density of sand and the confining pressure (Seed 1979). Resistance to liquefaction can be improved by increasing the density (densification), modifying the grain size distribution (grouting/mixing), stabilizing the soil

[1]Professor Emeritus, Department of Civil Engineering, Jawaharlal Nehru Technological University, Hyderabad 500 072, India. Email: madhav@iitk.ac.in
[2]Research Scholar, Department of Civil Engineering, Indian Institute of Science, Bangalore 560012, India. Email: amurali@civil.iisc.ernet.in

fabric (reinforcing), reducing the degree of saturation, dissipation of the excess pore pressures generated and interception of the propagation of excess pore pressures (drainage), etc. (Madhav and Arlekar, 2000).

A possible method of stabilizing a soil deposit susceptible to liquefaction is to install a system of gravel or rock drains (Seed and Booker 1977). Provision of sand drains/granular piles/stone columns is the most commonly adopted ground treatment methodology even for liquefaction mitigation and it has proved its effectiveness in many instances (Mitchell and Wentz 1991). Adalier and Elgamal (2004) reviewed the current state of the stone column technologies as a liquefaction countermeasure. Due to installation of gravel drains, the generated pore water pressures due to repeated loading may get dissipated almost as fast as they are generated. Thus granular piles are effective in mitigating liquefaction damage due to the drainage facility. In addition to the drainage effect, densification and reinforcement of the ambient soil around the rammed granular pile (RGP) should also be considered for total and better evaluation of the improvement.

Granular piles are of the displacement type and hence densify in situ ground during the process of installation (Madhav 2001). The effect of densification is manifested through an increase in the coefficient of earth pressure at rest and in the values of modulus of deformation of the soil (Ohbayashi et al. 1999). Densification by RGP causes increase in deformation moduli and decreases in the coefficients of permeability and volume change. The densification effect, however, decreases with distance from the center of the compaction point and may become negligible at the periphery of the unit cell. Thus, the coefficients of horizontal permeability, $k_h(r)$, and volume change, $m_v(r)$, of the soil around the granular can be considered to vary with distance, r, from the center of the granular pile. Moreover densified soils experience volume increase during shearing. Generation of very high negative pore pressures can be observed due to suppression of the tendency for dilation, which further enhances the liquefaction mitigation (Madhav and Arlekar 2000).

In this paper the pore pressure generation and dissipation of the treated ground under earthquake conditions is analyzed to quantify the densification effect of ground treatment with RGP and due to dilation of RGP. Theory of pore-water pressure generation and dissipation developed by Seed and Booker (1977) is applied, with some modifications for evaluating the densification and dilation effects of RGPs, to the analysis of columnar gravel drains under earthquake conditions.

RAMMED GRANULAR PILES

Ground improvement by means of granular piles/stone columns/geopiers, which is associated with partial substitution of the in–situ soil, originated in sixties. Granular piles ground provide increased bearing capacity, significant reduction in settlement, free drainage, increase of liquefaction resistance, etc. Granular piles are installed by vibro-compaction, vibro-replacement, cased bore hole (rammed stone columns/RGP) or by simple auger boring methods. RGP are installed into the ground by partial or full displacement methods and by ramming in stages, using a heavy falling weight, within a ‘pre-bored casing’ or ‘driven closed end casing’, retracting the casing pipe stepwise. In the latter case, driving of closed end tube itself densifies the surrounding soil.

Densification effect

Ramming action of the falling weight tends to ram the stone into the sides of the hole, which densifies more and reinforces the ground. Densification and reinforcement effects cause modifications in the properties of the in situ soil. This densification and modification in the soil parameters of the ground are not uniform over the entire zone of surrounding ground but is a function of the distance from the point of densification. During the process of installation of RGP, the soil adjacent to and in the vicinity of the point of treatment gets densified most. This densification effect decreases with the distance from the point of densification. Thus, the densification effect of the ground, due to the installation of granular pile, is maximum near the periphery of the granular pile and decreases with the distance from

the granular pile. Densification by RGP causes increase in deformation moduli and decrease in the coefficients of permeability and of volume change.

Sujatha (1998) analyzed several field test data and postulated linear and exponential variations of the stiffness of soil with distance as limits for the densification effect. Similar linear variations are considered for the reductions of flow and deformation parameters of the in situ soil (coefficients of permeability and volume change). This reduction will be most at the point of densification and decays with distance towards the periphery of the unit cell reaching the original in-situ values at the farthest end of the unit cell.

Linear variation of the flow parameters

A linear variation of the coefficient of horizontal permeability, k_h, with distance from the center of RGP is considered with k_h value becoming minimum at the edge of RGP (r = a) and maximum at the periphery of the unit cell (r = b) (Fig. 1). The general expression for the variation of the coefficient of permeability at a distance 'r' from the centre of the granular pile considering linear variation can be expressed as

$$k_h(r) = \left(\frac{k_{sb} - k_{sa}}{b - a} \right).(r - a) + k_{sa} \tag{1}$$

where k_{sa} and k_{sb} are the coefficients of permeability at the edge of RGB (r=a) and at the edge of the unit cell (r=b) respectively. Non-dimensionalising with k_{hi}, initial in-situ value of coefficient of permeability

$$R_k(r) = \left(\frac{R_{kb} - R_{ka}}{b - a} \right).(r - a) + R_{ka} \tag{2}$$

where $R_k = k_h/k_{hi}$, $R_{kb} = k_{sb}/k_{hi}$ and $R_{ka} = k_{sa}/k_{hi}$.

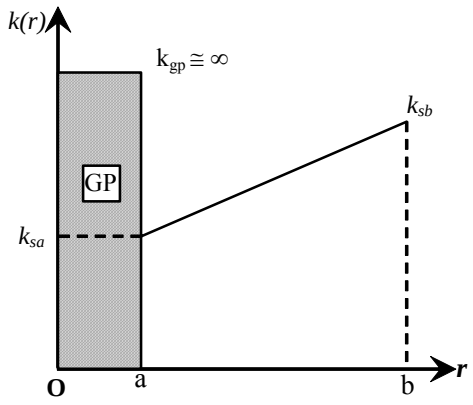

Figure 1. Variation of coefficient of permeability of soil with distance

Similarly, the expression for linear variation of coefficient of volume change, m_v, is

$$m_v(r) = \left(\frac{m_{vb} - m_{va}}{b - a} \right).(r - a) + m_{va} \tag{3}$$

where m_{va} and m_{vb} are respectively the coefficients at distances 'a' and 'b' from the centre. Non-dimensionalizing with 'm_{vi}', initial in situ value of coefficient of volume change, one gets

$$R_{mv}(r) = \left(\frac{R_{mb} - R_{ma}}{b - a} \right) . (r - a) + R_{ma} \tag{4}$$

Dilation effect

Figure 2(a) (Vaid et al. 1981) is a typical example of stress-strain behaviour of granular material under drained conditions in a simple shear test at different vertical stress conditions. While initially loose samples undergo volume decrease, dense samples experience volume increase (dilation) during shearing. The rate of dilation increases with relative density. The response of saturated sand under undrained triaxial conditions (Leonards 1962) can be seen in Figure 2(b). While positive pore pressures are generated in loose sands, generation of very high negative pore pressures can be observed due to suppression of the tendency for dilation.

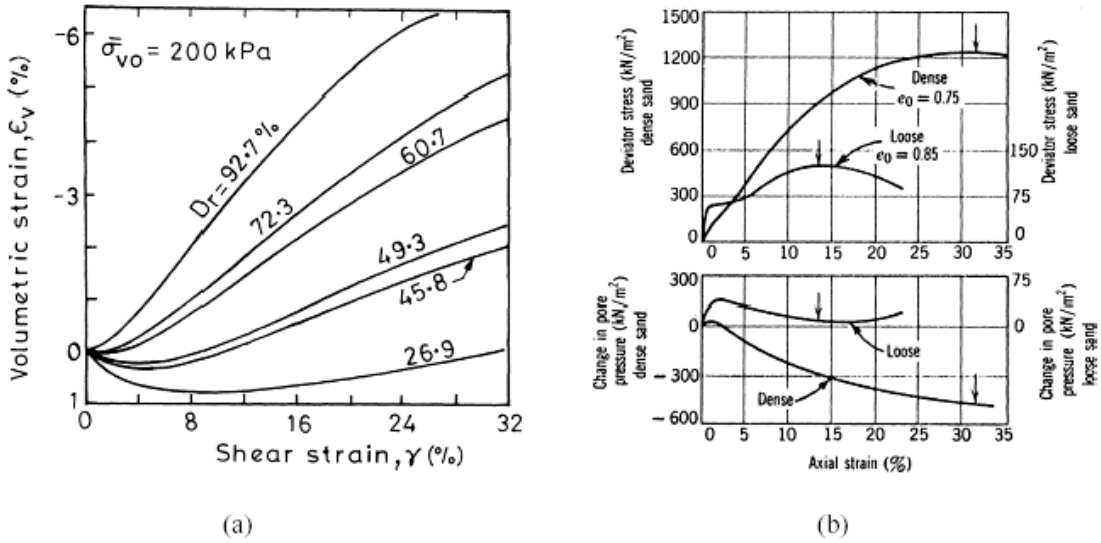

Figure 2. (a) Stress-strain behaviour for granular material under drained conditions (Vaid et al. 1981) (b) Response of saturated sand under undrained triaxial conditions (after Leonards 1962)

The dilation angle is one single parameter which can be readily obtained from both laboratory (drained triaxial or simple shear) and in situ (self-boring pressuremeter) tests, which can give a measure of the liquefaction resistance. Baez and Martin (1991) present an evaluation of the relative effectiveness of stone columns for the mitigation of liquefaction of soil. They also describe tests on footings on soil reinforced with stone columns, which have been used to calibrate a finite element program. The most interesting result obtained is that the stone columns experience an increase in effective stress simultaneously with the development of negative pore pressures. The effect of dilation of granular pile material on settlement response of granular pile treated ground has been investigated by Poorooshasb and Madhav (1985) and Van Impe and Madhav (1992). In the former, the response of a granular pile reinforced soil subjected to uniform loading through a relatively rigid raft is studied considering the granular pile material to follow the rigid plastic dilatant strain hardening postulates of Poorooshasb et al. (1966). The tendency for dilation is resisted by the soil, which offers larger interaction (confining) stresses. As a result, both the pile and the soil become stiffer with increasing applied stress. As a consequence of dilatant nature of the granular material, the settlement versus the intensity of loading curve exhibits a non-linear relation. The mechanical effect of dilatancy of granular material in increasing the stiffness of soft or loose soil deposits has been quantified in the above two works. The effect of dilatancy during undrained state that exists within a gravel drain/granular pile during a seismic event is also considered in the analysis.

SEED & BOOKER (1977) MODEL

In most practical cases, the horizontal permeability of sand/gravel deposit will be several times greater than its vertical permeability and usually the spacing between vertical drains is closer than the distance required for pore water to drain vertically towards the free surface. Furthermore, many natural deposits of sand are interspersed with narrow horizontal layers of relatively impermeable silt, which may severely inhibit vertical drainage. For these reasons, the dominant mechanism in the operation of a gravel drain system often is one of pure horizontal drainage (Seed and Booker 1977).

For flow into a gravel drain, assuming pure radial flow, and constant coefficients of permeability (k_h) and volume compressibility (m_v), the governing equation for the phenomenon can be written as (Seed and Booker 1977):

$$\frac{k_h}{\gamma_w . m_v}\left(\frac{1}{r}\frac{\partial u}{\partial r}+\frac{\partial^2 u}{\partial r^2}\right)=\frac{\partial u}{\partial t}-\frac{\partial u_g}{\partial N}.\frac{\partial N}{\partial t} \tag{5}$$

where u is the excess pore pressure at a radial distance r, from the centre, t is time, γ_w the unit weight of water, u_g = peak excess hydrostatic pore-water pressure generated by the earthquake; and

$$\frac{\partial u_g}{\partial N}=\frac{\sigma'_o}{\alpha\pi N_l}\frac{1}{\sin^{2\alpha-1}\left(\frac{\pi}{2}r_u\right)\cos\left(\frac{\pi}{2}r_u\right)} \tag{6}$$

where $r_u = u/\sigma'_o$ = the pore pressure ratio, σ'_o = the initial mean bulk effective stress for axi-symmetric conditions or the initial vertical effective stress for simple shear conditions; N_l is the number of cycles required to cause liquefaction and α = an empirical constant which is a function of the soil properties with typical average value of 0.7. The irregular cyclic loading induced by an earthquake is converted to an equivalent number, N_{eq}, of uniform cycles at an amplitude of 65% of the peak cyclic shear stress, i.e. $\tau_{cyc} = 0.65.\tau_{max,}$ occurring over a duration of time, t_d, and

$$\frac{\partial N}{\partial t}=\frac{N_{eq}}{t_d} \tag{7}$$

NEW MODEL CONSIDERING DENSIFICATION AND DILATION OF GROUND

The governing equation of Seed and Booker (1977) (Eq. 5) is modified to include the densification effect of RGP in dissipating the excess pore-water pressures. In the ground treated with RGP, coefficient of permeability (k_h) and coefficient of volume compressibility (m_v) are considered to depend on the distance, r, instead being constant values. Considering an element of soil, in polar coordinates as shown in Figure 3, laminar flow and using Darcy's law, the expression for the flow in radial direction is obtained as,

$$\frac{k(r)}{r}\frac{\partial h}{\partial r}+k(r)\frac{\partial^2 h}{\partial r^2}+\frac{\partial k(r)}{\partial r}\frac{\partial h}{\partial r}=\frac{S}{1+e}.\frac{\partial e}{\partial t} \tag{8}$$

From the stress-strain relations and definitions of coefficient of compressibility (a_v) and coefficient of volume change (m_v) and for S =1(fully saturated),

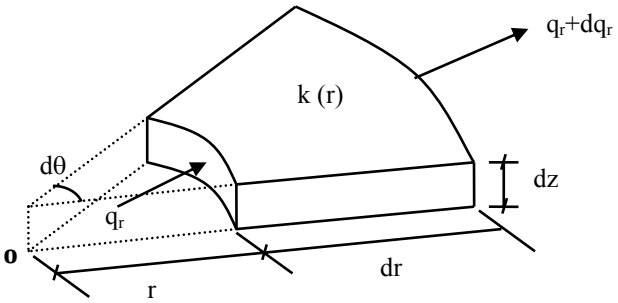

Figure 3. Flow through soil element.

$$\frac{1}{1+e}.\frac{\partial e}{\partial t}=\frac{m_v}{1+e}.\left(\frac{\partial u}{\partial t}-\frac{\partial \sigma}{\partial t}\right) \tag{9}$$

From Eq. 9 and with $h = u/\gamma_w$; (u = excess pore pressure; γ_w = unit weight of water) Eq. 9 is rewritten as:

$$\frac{k_h(r)}{\gamma_w.m_v(r)}\left(\frac{1}{r}\frac{\partial u}{\partial r}+\frac{\partial^2 u}{\partial r^2}\right)+\frac{1}{\gamma_w.m_v(r)}.\frac{\partial(k_h(r))}{\partial r}.\frac{\partial u}{\partial r}=\frac{\partial u}{\partial t}-\frac{\partial \sigma}{\partial t} \tag{10}$$

where $k_h(r)$ and $m_v(r)$ are defined in Eqs. (1) and (3) respectively.
Considering the rate of change of total stress ($\partial\sigma/\partial t$) as the rate of pore pressure generation

$$\frac{\partial u_g}{\partial t}=\frac{\partial u_g}{\partial N}.\frac{\partial N}{\partial t} \tag{11}$$

The final form of Eq. 10 is,

$$\frac{k_h(r)}{\gamma_w.m_v(r)}\left(\frac{1}{r}\frac{\partial u}{\partial r}+\frac{\partial^2 u}{\partial r^2}\right)+\frac{1}{\gamma_w.m_v(r)}.\frac{\partial(k_h(r))}{\partial r}.\frac{\partial u}{\partial r}=\frac{\partial u}{\partial t}-\frac{\partial u_g}{\partial N}.\frac{\partial N}{\partial t} \tag{12}$$

Eq. 12 is a more generalized equation considering all forms of non-homogeneity. In non-dimensional form, with normalized pore pressure $W = u/\sigma'_o$, which is the same as the pore pressure ratio r_u (Seed and Booker 1977) and $W_g = u_g/\sigma'_o$, Eq. 12 becomes

$$\frac{k_h(r)}{\gamma_w.m_v(r)}\left(\frac{1}{r}\frac{\partial W}{\partial r}+\frac{\partial^2 W}{\partial r^2}\right)+\frac{1}{\gamma_w.m_v(r)}.\frac{\partial(k_h(r))}{\partial r}.\frac{\partial W}{\partial r}=\frac{\partial W}{\partial t}-\frac{\partial W_g}{\partial N}.\frac{\partial N}{\partial t} \tag{13}$$

Non-dimensionalising the terms ‘r’ with ‘R’ (=r/b) and ‘t’ with ‘T’ (=t/t_d), Eq. 13 becomes

$$T_{bd}.\frac{R_k(R)}{R_{mv}(R)}\left(\frac{\partial^2 W}{\partial R^2}+\frac{1}{R}\frac{\partial W}{\partial R}\right)+\frac{T_{bd}.}{R_{mv}(R)}\frac{\partial(R_k(R))}{\partial R}.\frac{\partial W}{\partial R}=\frac{\partial W}{\partial T}-\frac{\partial W_g}{\partial N}N_{eq} \tag{14}$$

where

$$\frac{\partial W_g}{\partial N}=\frac{1}{\alpha\pi N_l}.\frac{1}{\sin^{2\alpha\text{-}1}\left(\frac{\pi}{2}r_u\right)\cos\left(\frac{\pi}{2}r_u\right)} \tag{15}$$

and $$T_{bd} = \left(\frac{k_{hi}}{\gamma_w} \frac{t_d}{m_{vi}} \right) . \frac{1}{b^2} \quad (16)$$

Eq. 14 is solved numerically using a finite difference approach, discretizing the unit cell radially into a number of elements, for the appropriate boundary and initial conditions (Murali Krishna 2003).

Boundary Conditions

The material in the drains is far more permeable than the surrounding sand layer (Gravel drain is infinitely permeable). If the effect of dilatancy of gravel drain is not considered the excess pore-water pressure in the drain is effectively zero i.e., at r = a or R = a/b, u = 0 or W= 0. Considering the dilation effect, since the granular piles tend to dilate under undrained conditions, they develop negative pore pressure which is estimated in a manner very similar to the estimation of positive pore pressure in loose sand deposits (Madhav and Arlekar 2000). Then the pore pressure at r = a is,

$$W_{g\ at\ r=a} = \left(\frac{u_g}{\sigma'_o} \right)_{at\ r=a} = -d_c \left(\frac{2}{\pi} \arcsin \left(\frac{N}{N_l} \right)^{1/2\alpha} \right) \quad (17)$$

where d_c is a constant that depends on the degree of dilatancy of the granular pile material and depends on the densification achieved during the installation of granular piles. At the outer boundary of the unit cell, due to symmetry, rate of pore-water pressure in the radial direction is zero, i.e.,

$$\text{at r = b or R = 1,} \quad \frac{\partial u}{\partial r} = 0 \text{ or } \frac{\partial W}{\partial R} = 0 \quad (18)$$

Initial Condition

At t = 0 or T = 0, pore pressures at all the nodes in the soil are equal to the average of pore water pressure generated over the initial time period of 'dt' (or 'dT'). i.e., average of pore-water pressure generated over an initial cycle interval, dN.

$$W_{g\ at\ T=0} = \left(\frac{u_g}{\sigma'_o} \right)_{at\ t=0} = \frac{1}{2} \left(\frac{2}{\pi} \arcsin \left(\frac{dN}{N_l} \right)^{1/2\alpha} \right) \quad (19)$$

RESULTS AND DISCUSSION

Under the assumption of purely radial flow, the pore pressure ratio, w= u /σ'_o, throughout the sand depends on the dimensionless parameters: a/b = a ratio representing the geometric configuration of the RGPs; N_{eq}/N_l = cyclic ratio characterizing the severity of the earthquake shaking in relation to the liquefaction characteristics of the sand; T_{bd}, relating the duration of the earthquake to the consolidation properties of the sand; α, a parameter characterizing the shape of the pore pressure generation curve. It is found that for many materials α = 0.7 fits the experimental data well, and this value is adopted (Seed and Booker, 1977); $R_k(r)$ & $R_{mv}(r)$, functions of radial distance, r, define the variations of coefficients of horizontal permeability and volume compressibility of the in situ soil respectively and d_c, a constant that depends on the degree of dilatancy of the granular material and depends on the densification achieved during the installation of granular piles.

If coefficients of permeability and volume change of the surrounding soil are unchanged and there is no dilation effect due to installation of RGP, the condition represents the 'No Densification & No Dilation' case. In this case the ambient soil will have the initial k_h and m_v (i.e., $R_{ka}= R_{kb}= R_{ma}= R_{mb}= 1$) and d_c = 0. The effect of a/b ratio on maximum pore water pressure is shown in Figure 4 for cyclic

ratio (N_{eq}/N_l) of 2 and a range of a/b (0.1 to 0.4) with T_{bd} value of 1. Maximum pore pressure ratio $W_{max}(T)$, i.e. maximum value of u/σ'_o throughout the layer is plotted against $T(t/t_d)$. These results are for no densification effect and agree closely with the results of Seed and Booker (1977). For cyclic ratio, (N_{eq}/N_l) equals to 2, if no drains are present (a/b = 0) the soil liquefies at $T_l = 1/(N_{eq}/N_l)$ i.e., at T = 0.5. For a/b = 0.1, initial liquefaction is deferred for a period of 'T' but eventually occurs at about T=0.6, the liquefied state, W_{max} = 1, continues until the end of the period of strong shaking. Thereafter pore-water pressure dissipates. It can be observed that at higher a/b values, initial liquefaction may be prevented as the maximum pore pressure ratio decreases with increase in a/b value.

Effect of cyclic ratio on maximum pore pressure ratio, without densification and dilation effects, is shown in Figure 5. A range of cyclic ratios, N_{eq}/N_l, 1 to 5 for a/b of 0.3 and T_{bd} of 1 is considered. As cyclic ratio increases, pore water pressure increases and leads to liquefaction depending on the generation and dissipation of pore pressures. The time at which the ground liquefies decreases with increase of cyclic ratio as per T_l (=1/(N_{eq}/N_l)). If attained, the liquefied state continues until the end of the period of strong shaking. i.e., T=1. Thereafter pore pressure ratio decreases gradually. It can be observed from Figure 5 that the peak value of W_{max} increased from about 0.27 to 0.52 for an increase in N_{eq}/N_l from 1 to 2. For N_{eq}/N_l values 3, 4 and 5, W_{max} reaches a value of one, at T of about 0.62, 0.35 and 0.24 respectively.

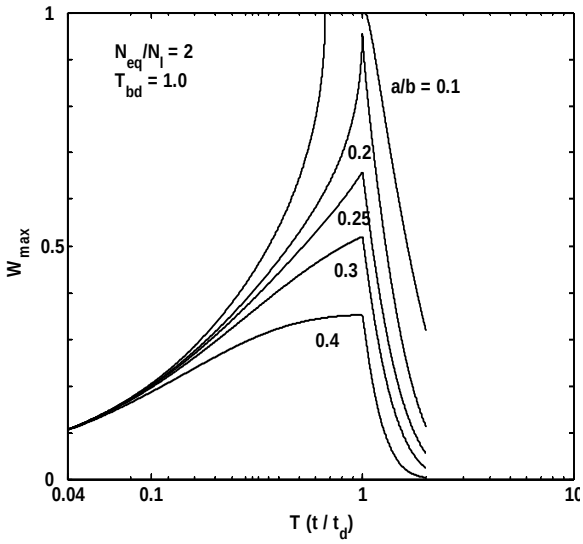

Figure 4. Effect of area ratio on W_{max} for 'No Densification & No Dilation' Case

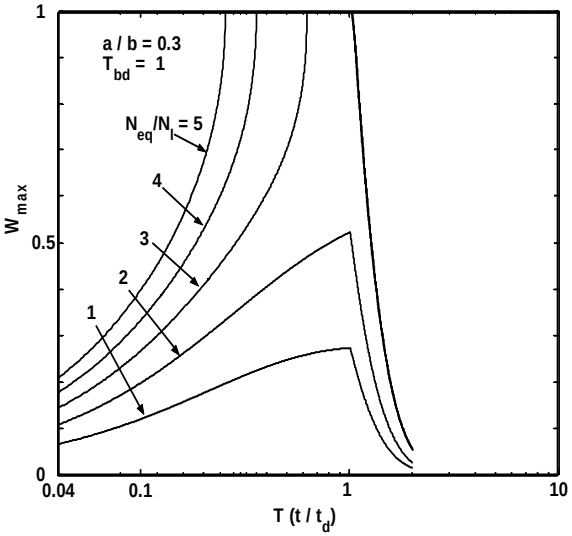

Figure 5. Effect of N_{eq}/N_l ratio on W_{max} for 'No Densification & No Dilation' Case

Densification effect, but with no dilation effect (d_c = 0), with respect to coefficient of volume change only (i.e., no change in coefficient of permeability (R_{ka}=R_{kb}= 1)) on maximum pore pressure ratio, W_{max}, is shown in Figures 6 and 7. Figure 6 shows the effect of densification at the near end, R_{ma}, on W_{max}, for no modification in the coefficient of volume change at the farthest end (R_{mb}=1). A range of R_{ma}(1-0.1) for T_{bd} = 1, a/b = 0.3 and N_{eq}/N_l = 2 is considered. It can be observed that W_{max} decreases with decrease in R_{ma}. Maximum pore pressure ratio, W_{max}, decreased from 0.525 to 0.375 for a decrease in R_{ma} from 1 to 0.1. The effect of densification at the farthest end (R_{mb}) is shown in Figure 7, considering the densification at the near end as R_{ma}=0.3. A range of R_{mb} from 1 to 0.5 for T_{bd} = 1, a/b = 0.3 and N_{eq}/N_l = 2 is considered. It can be observed that W_{max} decreases from 0.41 to 0.25 for a decrease in R_{mb} from 1 to 0.5. It can be concluded from Figures 6 and 7 that densification effects with respect to coefficient of volume change reduces the pore pressures and mitigates the liquefaction potential.

Densification effect in terms of coefficient of permeability only, i.e., no change in coefficient of volume change (R_{ma}=R_{mb}= 1), but with no dilation effect (d_c = 0), on maximum pore pressure ratio is

shown in Figures 8 and 9. The effect of densification at the near end, R_{ka}, on W_{max} for no modification in the coefficient of permeability at the farthest end (R_{kb}=1) is shown in Figure 8. A range of R_{ka} (1-0.5) for T_{bd} = 1, a/b = 0.3 and N_{eq}/N_l = 2 is considered. W_{max} increases from 0.525 to 0.675 for a decrease in R_{ka} from 1 to 0.8. For R_{ka}=0.6 the maximum pore pressure ratio reaches 1, i.e. the liquefied state. Further decrease in R_{ka} will reduce the time to attain the liquefaction state. Densification effect at the farthest end (R_{kb}) on maximum pore pressure ratio is shown in Figure 9 considering the densification at the near end as R_{ka}=0.6. A range of R_{kb} from 1 to 0.6 for T_{bd} = 1, a/b = 0.3 and N_{eq}/N_l = 2 is considered. It can be observed that the maximum pore pressure ratio is slightly affected by the densification at the farthest end, R_{kb}. It can be concluded from Figs. 8 and 9 that densification effects with respect to reduction in coefficient of permeability increase the pore pressures. This observation is revealing in that the densification effect with respect to coefficient of permeability alone results in a negative effect.

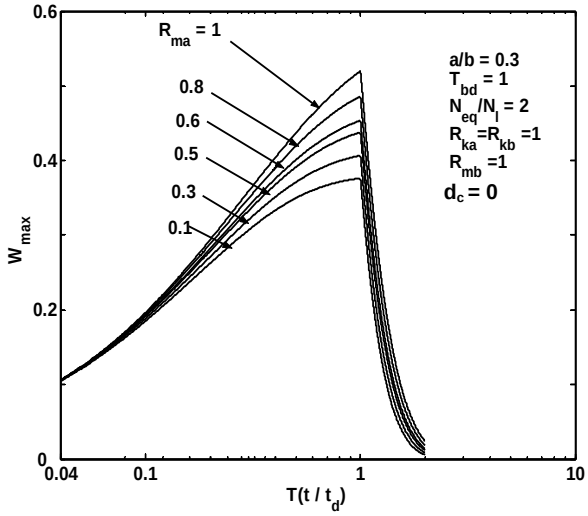

Figure 6. Effect of R_{ma} on W_{max}

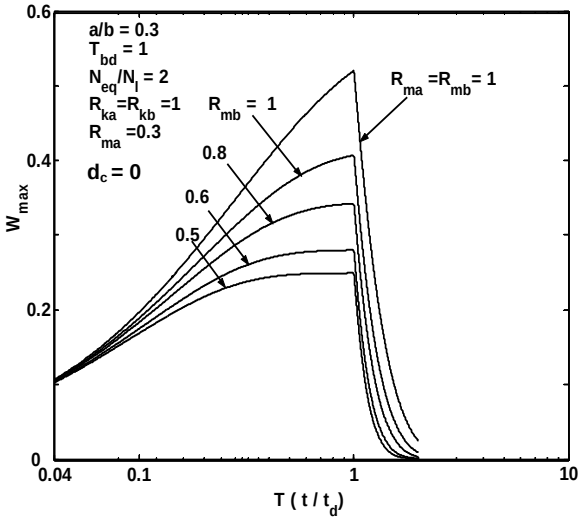

Figure 7. Effect of R_{mb} on W_{max}

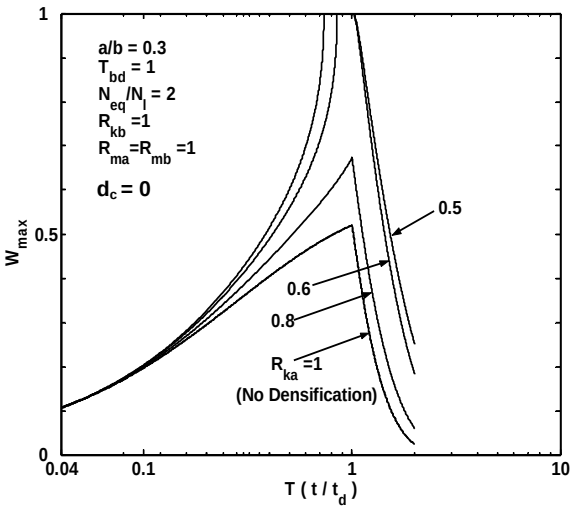

Figure 8. Effect of R_{ka} on W_{max}

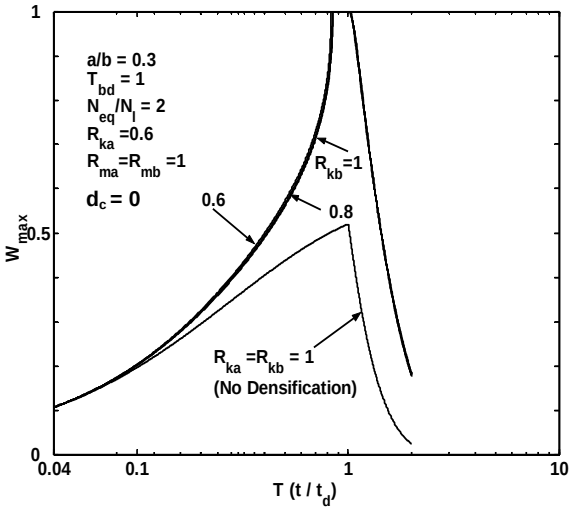

Figure 9. Effect of R_{kb} on W_{max}

Densification effect with respect to both the coefficients of permeability and volume change, but without dilation effect (d_c = 0), on W_{max} is shown in Figures 10 and 11. Figure 10 shows the densification effect on both the coefficients of permeability and volume change at near end on maximum pore pressure ratio, W_{max}. In this case the coefficients of permeability and volume change at the farthest end remain unaffected (R_{kb}= R_{mb}=1). A range of R_{ka} and R_{ma} (1-0.3) for T_{bd} = 1, a/b = 0.3 and (N_{eq}/N_l) = 2 is considered. The densification effect considered is the same for both R_{ka} and R_{ma}.

Maximum pore pressure ratio increases from 0.525 to 0.62 for a decrease in R_{ka} and R_{ma} from 1 to 0.8. W_{max} almost reaches 1, i.e. attains liquefaction state, at T =1 for R_{ka}=R_{ma}=0.6. Further decrease in R_{ka} and R_{ma} reduces the time corresponding to W_{max}=1. The effect of densification at the farthest end with respect to both coefficients of permeability (R_{kb}) and volume change (R_{mb}) on maximum pore pressure ratio, W_{max}, is shown in Figure 11, considering densification at the near end as R_{ka}= R_{ma}=0.6. The densification effect considered is the same for both R_{kb} and R_{mb} (1 – 0.7). W_{max} reaches 1 indicating liquefaction state, at T =1 for R_{kb}= R_{mb}=1 i.e. for no densification at the farthest end. Densification at the farthest end, i.e. reduction in R_{kb} and R_{mb} (from 1 to 0.7) reduces W_{max} (from about 1 to about 0.57), and thus establishes that liquefaction of ground is prevented by overall densification of the ground.

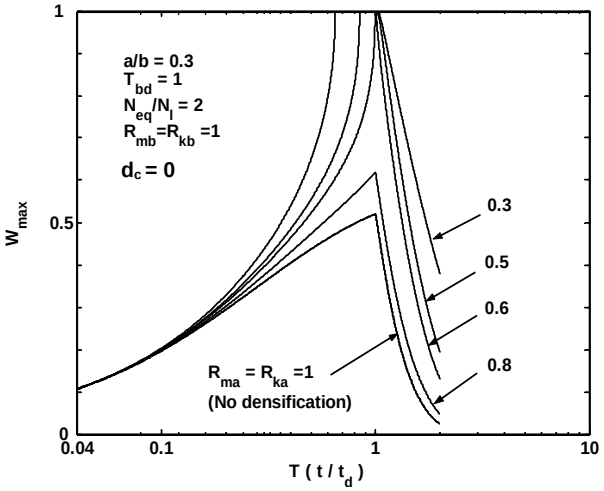

Figure 10. Effect of R_{ma} and R_{ka} on W_{max}

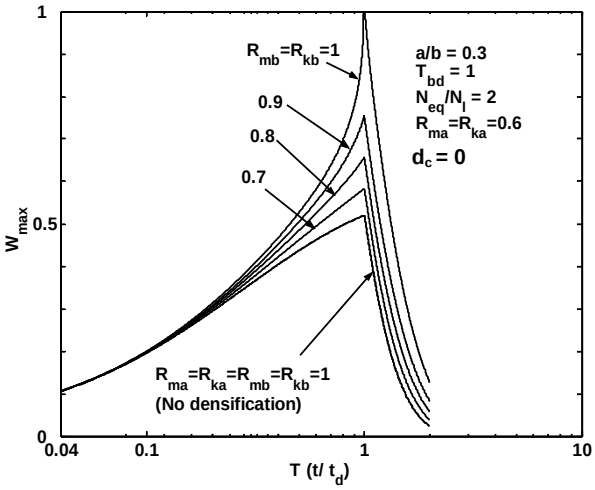

Figure 11. Effect of R_{mb} and R_{kb} on W_{max}

Effect of dilation alone, for no densification effect (i.e., R_{ka}= R_{kb}= R_{ma}= R_{mb}= 1), on maximum pore pressure ratio is presented in Figure 12. The effect of the dilation coefficient, d_c (0, 2 and 5), on the maximum pore pressure ratio for T_{bd} = 1, a/b = 0.2 and N_{eq}/N_l = 2, is shown in Figure 12. The negative pore pressures generated in the dilating gravel drain reduce the liquefaction induced pore pressures by permitting faster rates of dissipation. The curves for d_c equal to 2 and 5 indicate reductions in maximum pore pressures of the order of 13 and 17%. The maximum effect is obviously felt at t/t_d equal to 1.0.

Figure 13 provides the comparison of 'W_{max} versus T' curves for 'no dilation effect' (d_c = 0) and dilation effect with d_c = 2, along with the densification effect with respect to coefficient of permeability at the near end (R_{ka} = 1, 0.8 and 0.6). It is observed from the figure that the dilation effect reduced the maximum pore pressure ratios by 8.2, 5.2 and 4.3% for R_{ka} values of 0.6, 0.8 and 1 respectively implying that dilation effect is more for the case with higher densification effect.

CONCLUSIONS

An analysis of ground treated with gravel drains (stone columns) considering the effect of installation in densifying the ground and its dilation effect is proposed. Both the coefficients of volume change and permeability are considered to be affected due to densification. In fact they decrease because of

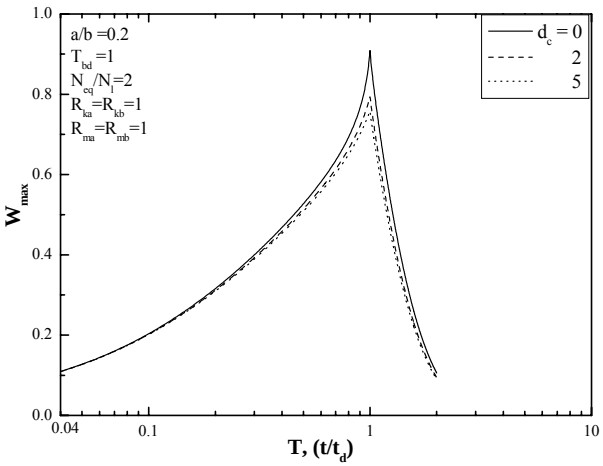

Figure 12. Maximum pore pressure ratio for different values of dilation coefficient

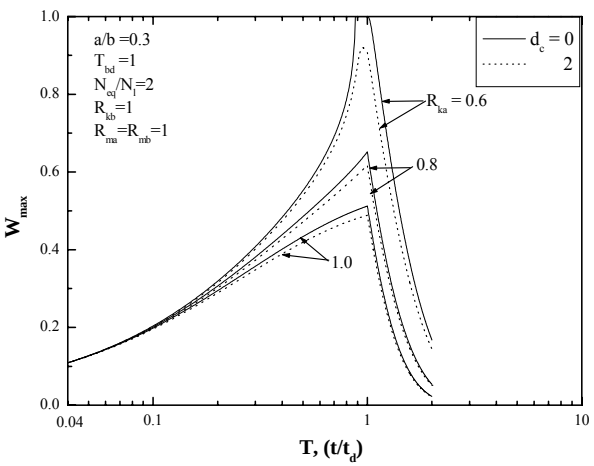

Figure 13. Effect of dilation and densification on W_{max}

densification. Dilation effect generates negative pore water pressures in the granular piles. Maximum pore pressure ratio decreases with closer spacing of gravel drains and increases with increase in cyclic ratio (N_{eq}/N_l). Densification effect on the coefficient of volume change alone is positive in that the maximum induced pore water pressure ratios get reduced. Densification effect on the coefficient of permeability alone increases the maximum pore water pressure ratios giving a negative effect.Densification effect on both coefficients of permeability and volume change gives a slightly negative or positive effect depending on the extent of densification. The negative pore pressures generated in dilating gravel drain reduce liquefaction induced pore pressures by permitting faster rates of dissipation, hence enhance liquefaction mitigation. The negative effect of the densification is balanced by the dilation effect thus proving the effectiveness of granular piles in the liquefaction mitigation.

REFERENCES

Adalier K and Elgamal A "Mitigation of liquefaction and associated ground deformations by stone columns," *Engineering Geology*, 72, No. 3-4, 275-291, 2004.

Baez JI and Martin GR "Quantitative evaluation of stone column technique for earthquake liquefaction mitigation," *10th World Conference on Earthquake Engineering*, 1477-1483, 1991.

Leonards GA (ed.), *Foundation Engineering*, McGraw-Hill, New York, 1962,

Madhav MR "Engineering of ground for earthquake disaster mitigation," *Proc. Indian Geotechnical Conference 2001*, Indore, India, 29-34, 2001.

Madhav MR and Arlekar JN "Dilation of granular piles in mitigating liquefaction of sand deposits," *12th World Conference Earthquake Engineering*, Auckland. No: 1035 (CD-ROM), 2000.

Martin WDL Finn and Seed HB "Fundamentals of liquefaction under cyclic loading," *J. of the Geotechnical Engineering Division*, ASCE, 101(GT5), 425-438, 1975.

Mitchell JK and Wentz FK "*Performance of improved ground during Loma Prieta earthquake*," Report No. EERC91/12, Earthquake Engineering Research Center, University of California, Berkeley, 1991.

Murali Krishna A "*Liquefaction mitigation of loose sand deposits by rammed granular piles*," M.Tech Thesis, Indian Institute of Technology, Kanpur, India, 2003.

Ohbayashi J, Harda , and Yamamoto M "Resistance against liquefaction of ground improved by sand compaction pile method," *Earthquake Geotechnical Engineering*, Seco e Pinto (ed.), Balkama, Rotterdam, 549-554, 1999.

Poorooshasb HB and Madhav MR "Application of rigid plastic dilatancy model for prediction of granular pile settlements," *4th International Conference on Numerical Methods in Geomechanics*, Nagoya, Japan, 1805-1808, 1985.

Poorooshasb HB, Holubec I and Sherbourne AW "Yielding and flow of sand in triaxial compression," *Canadian Geotechnical Journal*, 3, 179-190, 1966.

Seed HB "Soil liquefaction and cyclic mobility evaluation for level ground during earthquakes," *J. of the Geotechnical Enigineering Division*, ASCE, 105, No. 2, 201-255, 1979.

Seed HB and Booker JR "Stabilization of potentially liquefiable sand deposits using gravel drains," *J. of the Geotechnical Enigineering Division*, ASCE, 103, No. 7, 757-768, 1977.

Seed HB and Idriss IM. "*Ground Motions and Soil Liquefaction During Earthquakes*," Earthquake Engineering Research Institute, Oakland, California, 1982.

Sujatha KP "*Analysis of reinforcement and densification effects in improved ground*," M.Tech Thesis, Indian Institute of Technology, Kanpur, India, 1998.

Vaid Y, Byrne PM and Hughes JMO "Dilation angle and liquefaction potential," *Journal of Geotechnical Engineering*, ASCE, 103(7), 1003-1008, 1981.

Van Impe WF and Madhav MR "Analysis and settlement of dilating stone column reinforced soil," *Austrian Geotechnical Journal*, 137:114-121, 1992.